J Nanostruct 16(3): 3000-3012, Summer 2026

RESEARCH PAPER

Concentration-Dependent Modulation of Optical Properties in TiO_2 Nanoparticle-Treated HCT116 Colorectal Cancer Cells

Tamara Ail Nasser

Department of Basic Science, College of Dentistry, University of Babylon, Iraq

ARTICLE INFO

Article History:
Received 05 March 2026
Accepted 07 May 2026
Published 01 July 2026

Keywords:
Absorption coefficient
HCT116 colorectal cancer cells
Light–cell interaction
Optical properties
Refractive index
TiO_2 nanoparticles

ABSTRACT

The effectiveness of light-mediated therapies depends on cancer cells' optical response. We quantified the concentration-dependent optical behaviour of HCT116 cells exposed to TiO_2 nanoparticles in this study. To evaluate nanoparticle-induced photon propagation dynamics, diffuse reflectance and transmittance measurements in the visible range were taken and absorption coefficients and refractive index values computed. TiO_2 nanoparticle treatment caused a systematic change in optical properties. The absorbance coefficient and refractive index of treated cell suspensions were lower than untreated controls. The optical density of the cellular medium was modulated by nanoparticle concentration, as both the absorption coefficient and refractive index rose with nanoparticle concentration in the treated groups. These findings imply that dose-dependent nanoparticle incorporation alters photon attenuation and transmission routes, potentially affecting cell energy deposition. The measured data was used to theoretically derive quantum-optical parameters like photon energy, extinction coefficient, complex dielectric function, and optical conductivity to better describe light–matter interaction in the nanoparticle-treated cellular medium. Since TiO_2 has photocatalytic and photoactive capabilities, its optical modulation may impact light-based therapies that rely on controlled photon absorption and energy distribution for efficiency. The present study did not assess direct therapeutic endpoints, but the concentration-dependent optical and photonic trends show how engineered nanomaterials can tune cellular light–matter interactions, providing a photonic foundation for future nanoparticle-assisted cancer therapy research.

How to cite this article
Nasser T. TiO_2 Nanoparticle-Treated HCT116 Colorectal Cancer Cells. J Nanostruct, 2026; 16(3):3000-3012. DOI: 10.22052/JNS.2026.03.001

INTRODUCTION

Photon attenuation and redistribution in complicated heterogeneous mediums are controlled by inherent optical characteristics in biological cell systems. Microscale absorption, scattering, and refractive index variability cause diffuse reflectance and transmittance in cellular suspensions. The absorption coefficient measures photon energy dissipation in the medium, while refractive index changes control phase velocity and scattering. These characteristics characterise biological surroundings' effective optical signature and enable quantitative light–cell interaction analysis [1,2]. Recent biomedical photonics

* *Corresponding Author Email: den747.a.ali@uobabylon.edu.iq*

breakthroughs emphasise the role of artificial nanoparticles in optical property modulation. Nanoparticles change local electromagnetic field distributions and refractive index discontinuities in biological systems, affecting scattering cross-sections and attenuation pathways. Since nanoparticle density increases collective scattering and composite medium optical density, these effects are concentration-dependent [3,4]. Titanium dioxide (TiO_2) nanoparticles are important for their optical stability, high refractive index, and well-defined structural phases. The visible spectral area refractive index values for TiO_2 nanostructures vary between 2.4 and 2.7, depending on crystalline phase (anatase or rutile) and wavelength [3,5]. TiO_2 nanoparticles have been extensively studied for their light absorption, band gap, and structural-optical correlations, in addition to their function in photonic and optical materials research [3,6]. TiO_2's characteristics make it a promising choice for changing light propagation in biological mediums. Few studies have quantified how controlled modification in TiO_2 nanoparticle concentration affects optical parameters in cellular cancer models, despite well-documented intrinsic optical features. A system-level photonic interpretation of nanoparticle–cell interactions requires understanding concentration-dependent absorption coefficient and refractive index changes in nanoparticle-treated cell suspensions. HCT116 colorectal cancer cells are a reproducible and popular in vitro model for biomedical research. Systematic optical characterisation of TiO_2-treated HCT116 cell suspensions, including effective absorption coefficient and refractive index alterations from reflectance and transmittance studies, is still lacking. This study investigates the concentration-dependent adaptation of optical properties in TiO_2 nanoparticle-treated HCT116 cells in the visible spectrum (400-800 nm). Effective absorption coefficient and refractive index changes across nanoparticle concentrations were measured via diffuse reflectance and transmittance. This research uses composite system behaviour rather than inherent nanoparticle constants to establish a quantitative photonic framework for cancer cell nanoparticle-induced light propagation regulation.

MATERIALS AND METHODS

A study compared optical characteristics of HCT116 colorectal cancer cells with and without TiO_2 nanoparticles. Three phases comprised the methodology. TiO_2 nanoparticles were synthesised and characterised using DC sputtering to confirm shape and phase properties. To evaluate nanoparticle uniformity, scanning electron microscopy (SEM) examined surface appearance, particle dispersion, and structural features before biological use. Second, optical measurements were made on both untreated (control) and TiO_2NP-treated cell suspensions. In the visible range (400–800 nm), diffuse reflectance and transmittance spectra were produced, employing 473 nm as a typical excitation wavelength. Third, reflectance and transmittance data from UV–visible spectroscopy determined optical properties such effective absorption coefficient and refractive index changes.

Titanium Oxide (TiO_2NPs) Preparation

TiO_2NPs were made using DC sputtering. During sputtering, nanostructured TiO_2 deposits were formed by ejected material from a titanium target under controlled plasma conditions. Nanoparticulate material was carefully collected and processed into TiO_2 nanopowder for subsequent research. Use 100 mg of TiO_2 nanopowder and 100 mL of distilled water to generate a homogeneous suspension. Stir continuously at 2000 rpm at room temperature for 2 hours. The translucent liquid became milky with evenly scattered nanoparticles. The suspension was centrifuged at 12,000 rpm for 20 min to reduce agglomeration and stabilise dispersion. Extra biological and optical measurements were taken with the supernatant.

Structural Characterization of TiO_2 Nanoparticles

Before biological use, titanium dioxide nanoparticles were characterised for shape, particle size distribution, and crystalline phase. SEM examined surface morphology. Microscopic imaging showed quasi-spherical nanoparticles with homogeneous dispersion. An image-based investigation showed a 60-nm particle diameter for cellular interactions and visible light scattering. The crystal phases were determined by XRD. The anatase phase of TiO_2 was confirmed by diffraction patterns with peaks matching reference data. Anatase TiO_2's high refractive index (2.4 in visible spectrum) sets it apart from polymorphs like rutile for optical studies [7]. SEM and XRD validated TiO_2 nanoparticle form and phase before dispersion

and biological/optical evaluation.

Cell Culture and Nanoparticle Treatment

Human colorectal cancer HCT116 cells were optically evaluated in vitro. Cell culture took place in sterile RPMI growth media at 37 °C in a humidified 5% CO_2 environment. TiO_2 nanoparticle suspensions were freshly produced for each experiment to guarantee consistent dispersion. Separating treated and control cells. Untreated HCT116 cells were the control group, whereas treatment groups received TiO_2 nanoparticles at varied doses (31.25, 62.5, 125, 250, 500, and 1000 µg/mL) over 24 hours. The culture media was carefully collected and cells cleaned to remove loose nanoparticles following incubation. We focused optical measurements on cell-associated TiO_2 nanoparticles, not extracellular ones. Controlled-density cells were collected for optical examination.

Optical Measurements

An absorbance/transmittance double-beam UV-visible spectrophotometer measured 400-800 nm. Standard 1 cm optical path quartz cuvettes held samples. Before measurement, cell suspensions were adjusted to a density of around 1×10^6cells/mL. Refractive index readings should be interpreted with caution because reflectance values were acquired indirectly from spectrophotometric data rather than an integrating sphere. After 24-hour nanoparticle exposure and washing, treatment and control HCT116-cell suspensions showed identical cell densities before measurement. All groups had diffuse transmittance. Under identical experimental conditions, spectroscopic data showed reflectance-related optical behaviour. Background contributions were eliminated by baseline correction with appropriate reference media. Controlling all measurements decreased instrumental variability and ensured repeatability.

Optical Parameter Estimation

The Beer-Lambert law was utilised to estimate the effective absorption coefficient (µa) from measured transmittance spectra using first-order approximation. The Beer–Lambert law assumes a homogeneous, non-scattering medium, however cell suspensions with distributed nanoparticles may scatter significantly. Quoted µa values approximate apparent absorption coefficients, which may include scattering losses. The absorbance (A) was calculated:

$$A = -\log_{10}(T) \quad (1)$$

The absorption coefficient was estimated using:

$$\mu a = 2.303\, A / l \quad (2)$$

where l represents the optical path length of the cuvette (1 cm).

The refractive index (n) was calculated from reflectance data using Fresnel's equation under normal incidence. For non-absorbing or slightly absorbing materials at normal incidence, the relationship between reflectance (R) and refractive index (n) is: $R = [(n-1)/(n+1)]^2$, where $n = (1+\sqrt{R})/(1-\sqrt{R})$ This approach simplifies refractive index values in turbid cell suspensions by assuming specular reflection at a planar contact. R=measured reflectance. To evaluate concentration-dependent modification from TiO_2 nanoparticle treatment, all visible spectrum features (400-800nm) were studied. This study measured single experimental runs without biological duplicates. This study does not provide statistical metrics such as mean ± standard deviation, error bars, or significance tests (e.g., p-values). Since the findings are descriptive, future studies should use triplicate measurements and statistical analysis to draw quantitative conclusions.

Theoretical Calculations of Photonic and Quantum-Optical Parameters

To extend the experimental observations into a quantum-optical framework, a set of theoretical parameters was derived from the measured absorption coefficient (μ_a) and refractive index (n) at the wavelength of maximum optical response (λmax). These parameters characterize the light–matter interaction within the TiO_2-treated HCT116 cellular medium on a photonic and electronic level [15,16].

Photon energy (E_{ah})

The energy carried by a single photon at λmax was calculated using the Planck–Einstein relation:

$$E_{ph} = hc / \lambda \quad (3)$$

where h is Planck's constant (6.626×10^{-34} J·s) and c is the speed of light in vacuum (3×10^8 m/s). The practical form E_{ah}(eV) = 1240/λ(nm) was used

for direct conversion to electron-volt units.

Extinction coefficient (k)

The imaginary part of the complex refractive index, representing the attenuation of the electromagnetic wave within the medium, was estimated from:

$$k = \mu_a \lambda / 4\pi \quad (4)$$

Complex dielectric function ($\varepsilon = \varepsilon_1 + i\varepsilon_2$)

The real (ε_1) and imaginary (ε_2) components describe, respectively, the polarization response and the dissipative behavior of the medium:

$$\varepsilon_1 = n^2 - k^2, \qquad \varepsilon_2 = 2nk \quad (5)$$

Optical conductivity (σ_{opt})

This parameter quantifies the response of bound electronic charges to the oscillating electromagnetic field:

$$\sigma_{opt} = \alpha nc / 4\pi \quad (6)$$

where $\alpha = \mu_a$ is the absorption coefficient in cm^{-1}, and c is the speed of light in cm/s.

Appearing optical transition energy ($E\mathcal{F}$). The wavelength of maximum absorption ($E\mathcal{F} \approx hc/\lambda max$) was used to estimate the dominating electronic transition energy in the spectral window. The composite cellular–nanoparticle system's photonic transition is taken into account, as the intrinsic band gap of bulk TiO_2 (~3.2 eV for anatase) is in the UV region beyond the measuring

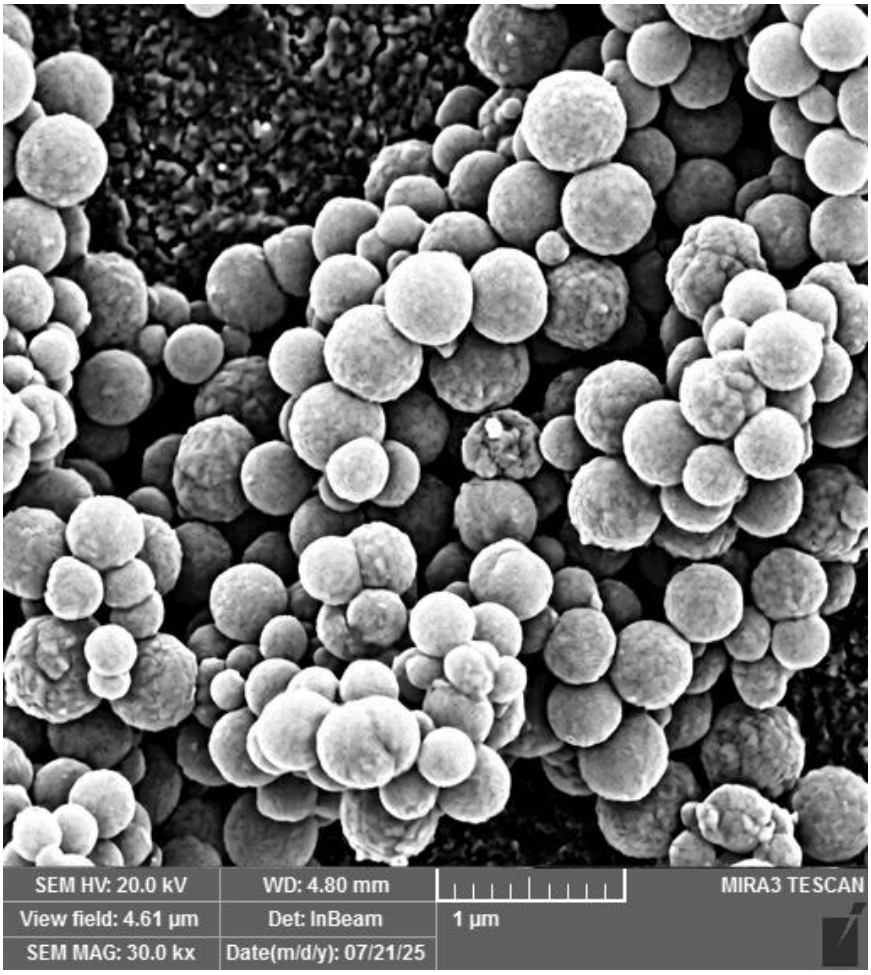

Fig. 1. SEM images of TiO_2 nanoparticles.

range.

RESULTS AND DISCUSSION

Structural Characterization of TiO_2 Nanoparticles

SEM examination showed that synthesised TiO_2 nanoparticles had a quasi-spherical shape and reasonably uniform spatial distribution. Agglomeration was low and particles were well-dispersed. Image-based tests showed an average particle diameter of 60 nm, indicating nanoscale dimensions adequate for optical interaction in cells.

XRD measurement revealed TiO_2 crystalline anatase phase. The diffraction pattern showed anatase structure peaks, indicating phase purity without secondary phases.

Transmittance Spectral Behavior

The transmittance spectra of control and TiO_2-treated HCT116 cell suspensions were measured in the visible range (400-800 nm). The control group had higher spectrum transmittance than treatment groups. Transmittance increased more in treated groups than controls. In the treated groups, transmittance decreased with higher TiO_2 nanoparticle concentration. Higher nanoparticle concentrations (500 and 1000 µg/mL) resulted in a greater fall in transmitted intensity, indicating increased optical attenuation in treated cellular suspensions. Light penetration and optical absorption are key to therapeutic applications. Thus, tissue optical characteristics are crucial to cancer detection and drug delivery. A UV–Vis spectrophotometer measured reflectance and transmittance. In Fig. 3, reflectance (R) and transmittance (T) measurements are given, with findings in Tables 1 and 2.

Results indicate differing reflectance and transmittance levels in untreated and TiO_2NP-treated HCT116 cells. A mathematical model based on the Beer–Lambert law and Fresnel equations estimated the absorption coefficient and refractive index using reflectance and transmittance measurements. Fig. 4 shows measurements, while

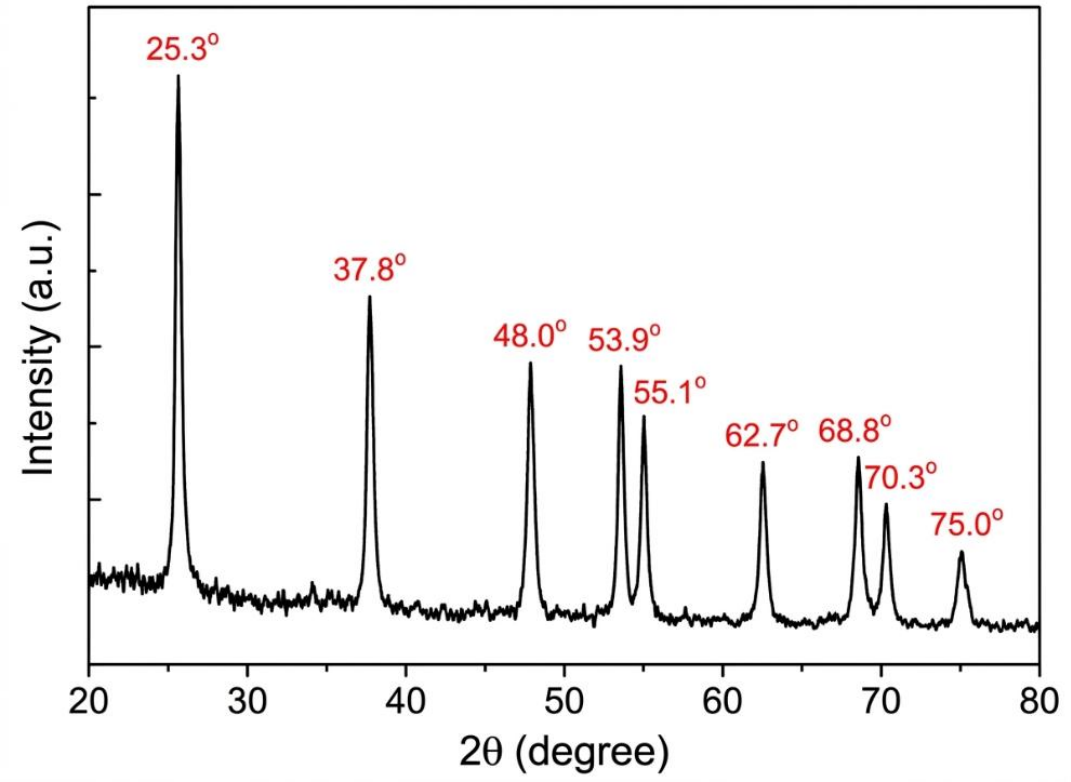

Fig. 2. XRD diffraction pattern confirming the anatase crystalline phase of the synthesized TiO_2 nanoparticles used in this study.

Tables 3 and 4 provide results. In the treated groups, increasing nanoparticle concentration increases absorption coefficient and refractive index values, although all values remain lower than the untreated control.

Derived Photonic and Quantum-Optical Parameters

Using experimentally obtained absorption coefficient (μ_a) and refractive index (n), theoretical photonic parameters were derived using equations (1)–(4) in Section 2.6. Included parameters: photon energy (E_{ah}), extinction coefficient (k), complex dielectric function (ε_1, ε_2), and optical conductivity (σ_{opt}). The calculated values are in Table 5.

The computed photon energy (E_{ah}) at λmax ranges from 2.376 to 2.408 eV for all samples, corresponding to the visible spectrum's green area. The observed optical response in anatase TiO_2 is due to sub-gap absorption within the composite

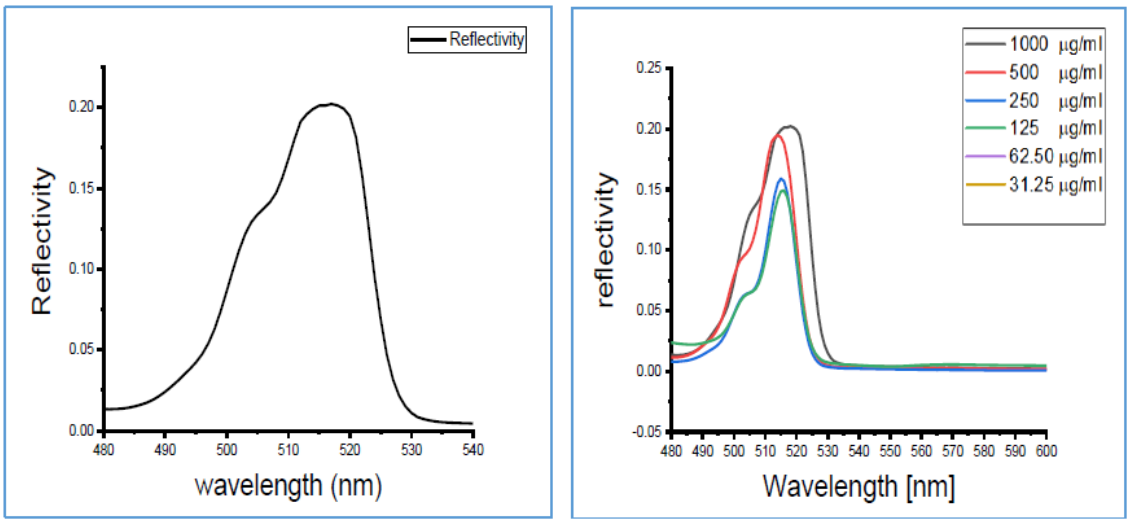

Fig. 3. Transmittance and reflectance spectra of HCT116 colon cancer cells with and without TiO_2 nanoparticle treatment.

Table 1. Reflectance and transmittance measurements of untreated HCT116 cells (control group).

Measurements	Wavelength (nm)	Cell Culture
R	519	0.2
T	522	0.45

Table 2. Reflectance and transmittance measurements of HCT116 cells treated with TiO_2NPs.

Concentration (µg/mL)	λmax (nm)	T	R
1000	519	0.459	0.2
500	514	0.52	0.18
250	515	0.669	0.16
125	516	0.672	0.15
62.5	516	0.671	0.15
31.25	516	0.671	0.15

cellular–nanoparticle system, not electronic changes in TiO_2. Sub-gap absorption is linked to defect states, surface trap levels, and oxygen-vacancy-related midgap states in nanomaterials [17,18]. The TiO_2 dose increased the extinction coefficient (k) from 1.558×10^{-2} in control to 1.483 at 1000 µg/mL, after initially decreasing to 0.617. In the cellular medium, nanoparticle concentration considerably affects electromagnetic wave attenuation. This pattern fits the absorption coefficient. Both dielectric function components (ε_1, ε_2) increased concentration-dependently in treated groups, demonstrating higher polarisation response and dissipative behaviour with increasing nanoparticle load [15,19]. The optical conductivity (σ_{opt}) showed a concentration-dependent increase from 6.446×10^{12} s^{-1} at low concentration to 18.32×10^{12} s^{-1} at 1000 µg/mL. Rising TiO_2 concentration leads to higher polarisable nanoparticle–cell interface density, resulting in greater bound charge responsiveness to electromagnetic fields. These quantum-optical characteristics describe how TiO_2 nanoparticles affect light-matter interaction in HCT116 cellular suspensions, supporting the dose-dependent modulation found in primary optical studies [16,20].

Observing the Glowing Light of the Synthesized Nanoparticle During the Photomicrographs

Fig. 5 displays HCT116 colon cancer cell optical micrographs taken under an inverted microscope. The glowing effect in cells treated with TiO_2NPs may be due to the optical scattering and reflective properties of the nanoparticles within the cell membrane. No direct cell viability experiment (such as MTT, XTT, or Trypan blue exclusion)

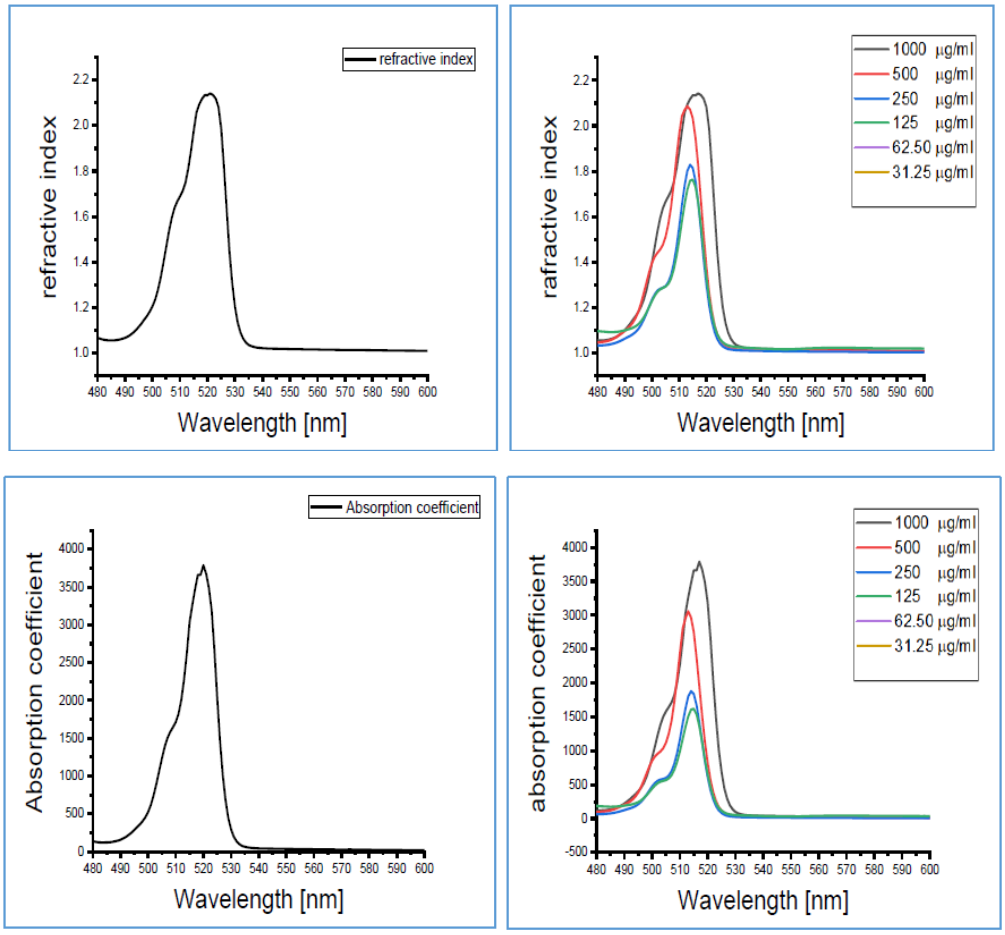

Fig. 4. Absorption coefficient and refractive index of HCT116 colon cancer cells with and without TiO_2 nanoparticle treatment.

was performed in this work, hence microscopic findings cannot be used to quantify cytotoxicity. Previous research suggests that TiO_2NPs may affect cancer cells based on size and concentration [14]. The morphological changes in Fig. 5 suggest dose-dependent effects, but future studies need specialised viability assays to quantify these findings.

This work shows that TiO_2 nanoparticles considerably impact the optical properties of cellular suspensions. These effects can be explained by photons interacting with nanoscale structures in the biological environment. SEM examination showed that the nanoparticles average 60 nm in diameter. Due to their high surface-to-volume ratio, particles in this size range interact well with visible light. This structural feature increases photon–particle interaction, which impacts light transmission across the cellular medium. XRD showed that the nanoparticles were mostly anatase crystalline. The anatase phase is known for its superior optical and photocatalytic properties compared to other TiO_2 phases. This structural characteristic increases photon absorption and scattering, changing biological samples' optical sensitivity. As nanoparticle concentration grew, transmission intensity decreased in this study's transmittance spectrum. Two main mechanisms explain this behaviour. Nanoparticles increase photon scattering in suspension. Additionally, nanoparticles can absorb some radiation. Light intensity decreases due to dispersion and absorption. Additionally, nanoparticle concentration clearly affected absorption coefficient values. Note that all treated groups had lower μa values than the untreated control. Higher TiO_2 concentrations in treated groups led to increased μa values over the tested spectral area. This shows that while sample preparation and nanoparticle treatment modify the optical environment, nanoparticles modulate effective attenuation in the treated cellular medium dose-dependently. Previous investigations using nanostructured materials

Table 3. Absorption coefficient and refractive index of untreated HCT116 cells (control group).

Measurements	Wavelength (nm)	Cell Culture
Absorption Coefficient	522	3750
Refractive Index	520	2.17

Table 4. Absorption coefficient and refractive index of HCT116 cells treated with TiO_2NPs.

Concentration (μg/mL)	λmax (nm)	Absorption Coefficient	Refractive Index
1000	522	3570	2.15
500	515	3137	2.1
250	517	1722	1.84
125	517	1506	1.81
62.5	517	1500	1.8
31.25	517	1500	1.8

Table 5. Theoretically derived photonic and quantum-optical parameters for control and TiO_2NP-treated HCT116 cells at λmax.

Conc. (μg/mL)	λmax (nm)	E_{ah} (eV)	k ($\times10^{-2}$)	ε_1	ε_2 ($\times10^{-2}$)	σ_{opt} ($\times10^{12}$ s^{-1})
Control	522	2.376	1.558	4.709	6.761	19.43
1000	522	2.376	1.483	4.622	6.377	18.32
500	515	2.408	1.286	4.410	5.400	15.73
250	517	2.399	0.708	3.386	2.607	7.564
125	517	2.399	0.620	3.276	2.243	6.508
62.5	517	2.399	0.617	3.240	2.222	6.446
31.25	517	2.399	0.617	3.240	2.222	6.446

in biological systems showed concentration-dependent variations in optical attenuation. Refractive index estimation showed measured differences between control and treatment samples. The suspension's effective optical density may explain treated groups' higher refractive index. Dispersed nanoparticles in biological media create dielectrically distinct areas. Heterogeneity

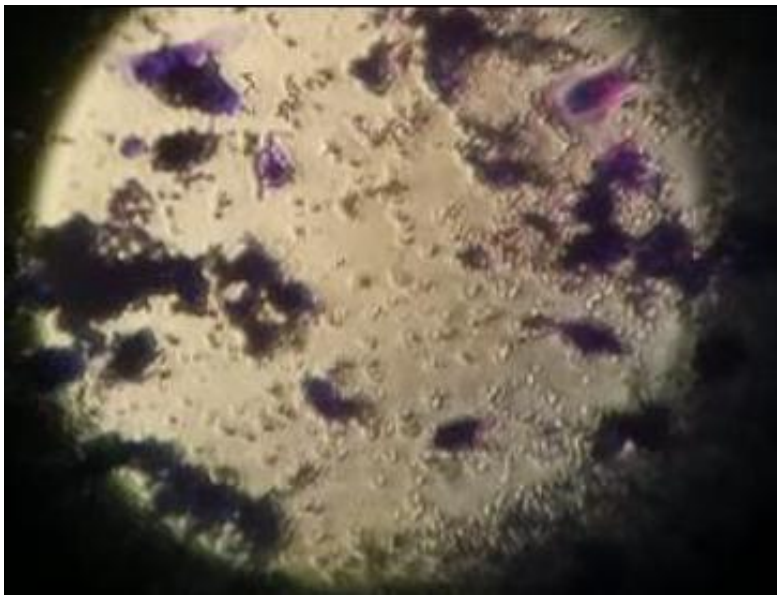

Fig. 5. Morphological observations of HCT116 colon cancer cells after exposure to different concentrations of TiO_2 nanoparticles for 24 hours.

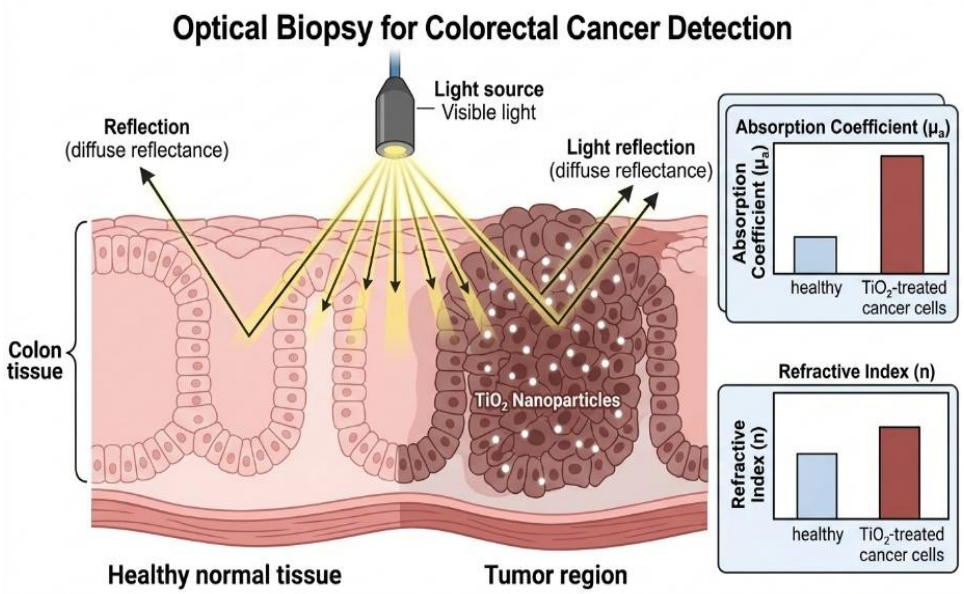

Fig. 6. Schematic illustration of optical biopsy for colorectal cancer detection, showing how the absorption coefficient and refractive index contrast between TiO_2-treated HCT116 cells and healthy colonic tissue can be exploited through diffuse reflectance spectroscopy to non-invasively localize tumor regions.

affects the system's refractive properties and light propagation. The theoretically obtained optical parameters in Section 3.3 illuminate the physical mechanics. The photon energy at λmax (2.38–2.41 eV) is below the inherent band gap of anatase TiO_2 (~3.2 eV), suggesting that the major absorption mechanism in the spectral window does not involve direct band-to-band transitions in crystalline TiO_2. In nanostructured anatase, sub-gap transitions involving oxygen-vacancy midgap states, surface trap levels, and defect-induced energy states likely control the optical response

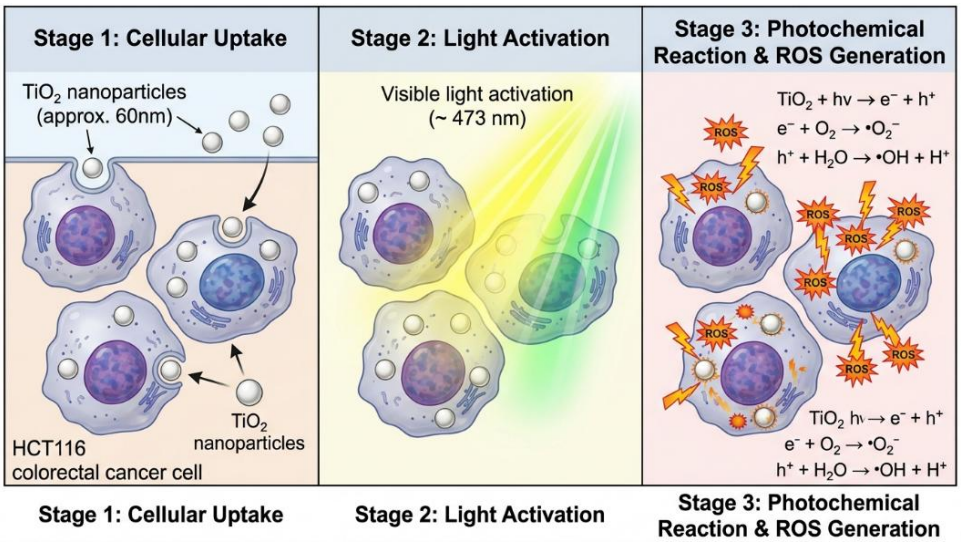

Fig. 7. Proposed mechanism of photodynamic therapy (PDT) using TiO_2 nanoparticles in HCT116 colorectal cancer cells. Upon visible-light activation, internalized nanoparticles generate reactive oxygen species (ROS) that induce selective oxidative damage, with therapeutic efficiency scaling with the concentration-dependent absorption coefficient derived in this study.

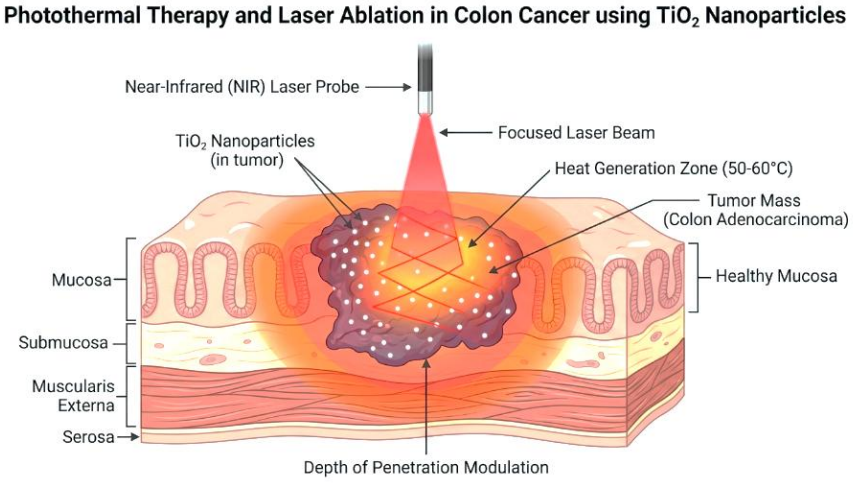

Fig. 8. Schematic representation of photothermal therapy and laser-assisted tumor ablation. The refractive-index modulation of TiO_2-treated cellular medium governs the optical penetration depth and enables localized heating of the tumor region while sparing surrounding healthy tissue.

[17,18,21]. Increased TiO_2 concentration leads to higher attenuation coefficient (k) and imaginary dielectric component (ε_2), suggesting greater photon energy dissipation. Enhanced polarisation response of the composite system is indicated by an increase in the real dielectric component (ε_1). The composite's optical conductivity (σ_{opt}) increased from 6.4×10^{12} s^{-1} at low concentration to 18.3×10^{12} s^{-1} at 1000 µg/mL, indicating that higher nanoparticle densities improve the composite's electromagnetic response. These quantum-optical parameters rationalise experimental results and link concentration-dependent optical modulation to cellular photonic and electrical systems. Other causes for optical changes include nanoparticle-biological interactions. Nanoparticles of TiO_2 can affect the optical environment by interacting with cell membranes or intracellular structures. Cellular components and media affect scattering and refractive index contrast. The optical characteristics of the cellular solution change when TiO_2 nanoparticles are added. Lower transmittance, increased absorption coefficient, and refractive index change. Nanoparticle-assisted optical methods may detect nanoparticle–cell interactions due to optical changes.

Potential Biomedical Applications

This study shows concentration-dependent optical modulation, which has applications in biological photonics and light-based cancer treatment. The difference in absorption coefficient and refractive index between untreated and TiO_2-treated HCT116 cells enables optical biopsy and non-invasive tumour detection. Diffuse reflectance spectroscopy can distinguish cancerous tissue from healthy tissue. Early colorectal cancer diagnosis improves clinical outcomes, making optical contrast useful [22,23,24].

In photodynamic therapy (PDT), TiO_2 nanoparticles can be used as photosensitisers to generate reactive oxygen species. The concentration-dependent increase in absorption coefficient can help determine optimal nanoparticle dosing and excitation wavelength. Optimising photon energy deposition within target cancer cells while minimising off-target exposure to healthy tissue improves treatment selectivity and reduces side effects [25-27].

Laser-assisted tumour ablation and photothermal therapy are also affected by refractive index modulation. To heat tumour areas without overheating neighbouring anatomical

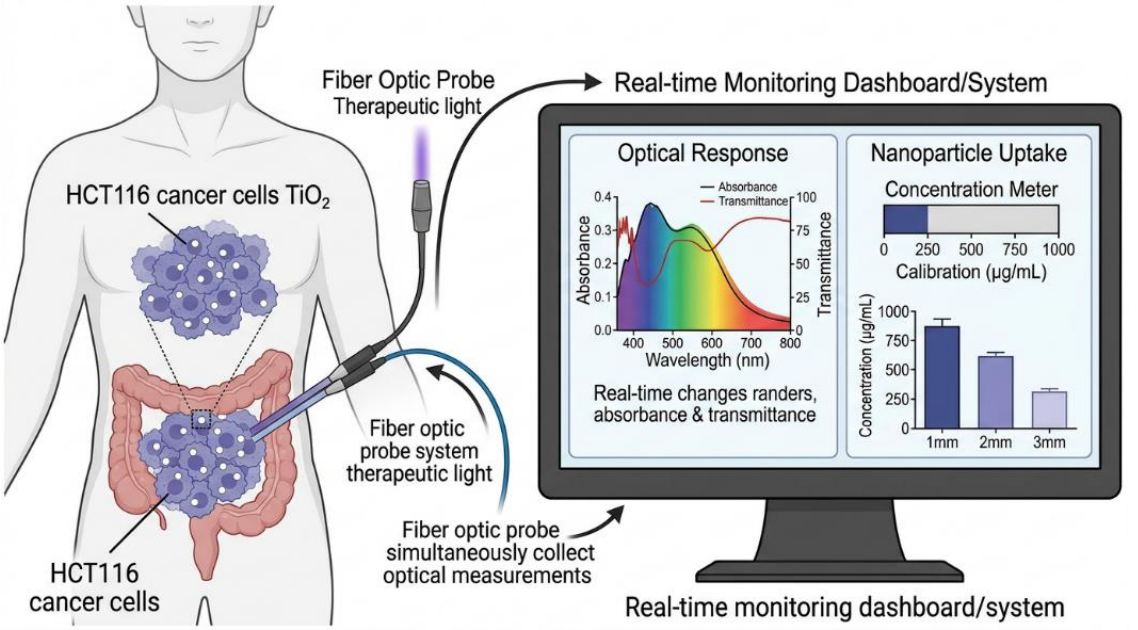

Fig. 9. Conceptual diagram of a nanoparticle-based optical dosimeter for real-time treatment monitoring. Continuous measurement of the optical response of TiO_2-treated HCT116 cells provides feedback on nanoparticle uptake, drug delivery, and therapeutic progression during clinical intervention.

structures, the effective optical density of the cellular medium can be controlled to precisely tune therapeutic light penetration depth. Thus, this study's dose-response pattern can influence colorectal cancer near-infrared laser treatment planning [28,29].

The illuminating effect in inverted microscopy suggests TiO_2 nanoparticles could be used as contrast agents for fluorescence-based and dark-field optical imaging of colorectal cancer cells, facilitating early diagnosis and image-guided surgery. The quantitative framework linking nanoparticle concentration to measurable optical parameters can be used to design nanoparticle-based optical dosimeters which use the local optical response as a real-time feedback signal to monitor drug delivery, tumour response, and treatment progression during clinical intervention [30].

CONCLUSION

The study examined the impact of TiO_2 nanoparticles on the optical properties of cellular suspensions by visible spectrophotometric measurements. SEM and XRD measurements confirmed the anatase crystalline phase and an average particle size of 60 nm for the nanoparticles. Experimental observations show that TiO_2 nanoparticles alter the optical response of the materials. As nanoparticle concentration increased, transmittance dropped, indicating higher light attenuation in the cellular medium. Nanoparticles increase absorption and scattering, causing this behaviour. Nanoparticle concentration clearly affected optical characteristics including absorption coefficient and refractive index. The absorption coefficient and refractive index of all treated groups were lower than the untreated control, but as nanoparticle concentration increased, these metrics increased. Research indicates that TiO_2 nanoparticles alter the optical characteristics of cells and impact light propagation in the biological medium in a concentration-dependent manner. These findings suggest nanostructured materials may affect biological systems' optical properties. The theoretically determined quantum-optical parameters—photon energy, extinction coefficient, complex dielectric function, and optical conductivity—matched experimental trends and provided a photonic explanation of nanoparticle-induced modulation. The changes in optical properties may help investigate nanoparticle–cell interactions and create nanoparticle-assisted optical diagnostic methods.

CONFLICT OF INTEREST

The authors declare that there is no conflict of interests regarding the publication of this manuscript.

REFERENCES

1. Hamdy O, Abdel-Salam Z, Abdel-Harith M. Optical Characterization of Biological Tissues Based on Fluorescence, Absorption, and Scattering Properties. Diagnostics. 2022;12(11):2846.
2. Re R, Spinelli L, Martelli F, Di Sieno L, Bargigia I, Amendola C, et al. A review on time domain diffuse optics: principles and applications on human biological tissues. La Rivista del Nuovo Cimento. 2025;48(3):157-239.
3. Alothoum MAS. A Review of the Synthesis, Structural, and Optical Properties of TiO_2 Nanoparticles: Current State of the Art and Potential Applications. Crystals. 2025;15(11):944.
4. Shahin A. Modeling of diffuse reflectance for a two layered medium: A Monte-Carlo study. Results in Optics. 2024;15:100634.
5. Bougdid Y, Kulkarni G, Chenard F, Sugrim CJ, Kumar R, Kar A. Optical properties of transparent TiO2 films by sintering anatase nanoparticles with a CO_2 laser. Opt Mater. 2024;156:115969.
6. Investigation of the Optical and Structural Properties of Cr^{3+}-Doped Al_2O_3 and $ZnAl_2O_4$ Nanoparticles Synthesized by Sol–Gel Method. Nanosistemi, Nanomateriali, Nanotehnologii. 2022;20(2).
7. Hanaor DAH, Sorrell CC. Review of the anatase to rutile phase transformation. Journal of Materials Science. 2010;46(4):855-874.
8. Vikas, Kumar R, Soni S. Quantitative study of concentration-dependent optical characteristics of nanoparticle-embedded tumor. Applied Nanoscience. 2021;11(10):2589-2597.
9. Enderlein J, Gregor I, Patra D, Fitter J. Art and Artefacts of Fluorescence Correlation Spectroscopy. Curr Pharm Biotechnol. 2004;5(2):155-161.
10. Fernández-Suárez M, Ting AY. Fluorescent probes for super-resolution imaging in living cells. Nature Reviews Molecular Cell Biology. 2008;9(12):929-943.
11. Koochesfahani M, Cohn R, MacKinnon C, Koochesfahani M. Simultaneous whole-field measurements of velocity and concentration fields using a combination of MTV and LIF. Meas Sci Technol. 2000;11(9):1289-1300.
12. Iles A, Pamme N. Sputtering for Film Deposition. Encyclopedia of Microfluidics and Nanofluidics: Springer US; 2014. p. 1-9.
13. Marpu SB, Benton EN. Shining Light on Chitosan: A Review on the Usage of Chitosan for Photonics and Nanomaterials Research. Int J Mol Sci. 2018;19(6):1795.
14. Geladi P, Manley M. Near-Infrared Hyperspectral Imaging in Food Research. Raman, Infrared, and Near-Infrared Chemical Imaging: Wiley; 2010. p. 243-260.
15. Wooten F. Maxwell's Equations and the Dielectric Function. Optical Properties of Solids: Elsevier; 1972. p. 15-41. http://

dx.doi.org/10.1016/b978-0-12-763450-0.50007-6
16. Dressel M, Grüner G. Electrodynamics of Solids: Cambridge University Press; 2002 2002/01/17.
17. Pan X, Yang M-Q, Fu X, Zhang N, Xu Y-J. Defective TiO_2 with oxygen vacancies: synthesis, properties and photocatalytic applications. Nanoscale. 2013;5(9):3601.
18. Bak T, Bogdanoff P, Fiechter S, Nowotny J. Defect engineering of titanium dioxide: full defect disorder. Advances in Applied Ceramics. 2012;111(1-2):62-71.
19. Perkins D. Euan Cameron, The European Reformation. 2nd Ed. Oxford/New York/Auckland, Oxford University Press 2012 Cameron Euan The European Reformation. 2nd Ed. 2012 Oxford University Press Oxford/New York/Auckland £ 24,99. Historische Zeitschrift. 2013;296(1):196.
20. Yu J, Low J, Xiao W, Zhou P, Jaroniec M. Enhanced Photocatalytic CO_2-Reduction Activity of Anatase TiO_2 by Coexposed {001} and {101} Facets. Journal of the American Chemical Society. 2014;136(25):8839-8842.
21. Khan MM, Ansari SA, Pradhan D, Ansari MO, Han DH, Lee J, et al. Band gap engineered TiO_2 nanoparticles for visible light induced photoelectrochemical and photocatalytic studies. J Mater Chem A. 2014;2(3):637-644.
22. Bigio IJ, Bown SG. Spectrroscopic Sensing of Cancer and Cancer Therapy: Current Status of Translational Research. Cancer Biology & Therapy. 2004;3(3):259-267.
23. Jacques SL. Optical properties of biological tissues: a review. Phys Med Biol. 2013;58(11):R37-R61.
24. Bashkatov AN, Genina EA, Kochubey VI, Rubtsov VS, Kolesnikova EA, Tuchin VV. Optical properties of human colon tissues in the 350 – 2500 nm spectral range. Quantum Electronics. 2014;44(8):779-784.
25. Rozhkova EA, Ulasov I, Lai B, Dimitrijevic NM, Lesniak MS, Rajh T. A High-Performance Nanobio Photocatalyst for Targeted Brain Cancer Therapy. Nano Lett. 2009;9(9):3337-3342.
26. Ziental D, Czarczynska-Goslinska B, Mlynarczyk DT, Glowacka-Sobotta A, Stanisz B, Goslinski T, et al. Titanium Dioxide Nanoparticles: Prospects and Applications in Medicine. Nanomaterials. 2020;10(2):387.
27. Fujishima A, Rao TN, Tryk DA. Titanium dioxide photocatalysis. Journal of Photochemistry and Photobiology C: Photochemistry Reviews. 2000;1(1):1-21.
28. Jaque D, Martínez Maestro L, del Rosal B, Haro-Gonzalez P, Benayas A, Plaza JL, et al. Nanoparticles for photothermal therapies. Nanoscale. 2014;6(16):9494-9530.
29. Chen J, Ning C, Zhou Z, Yu P, Zhu Y, Tan G, et al. Nanomaterials as photothermal therapeutic agents. Prog Mater Sci. 2019;99:1-26.
30. Wilson BC, Patterson MS. The physics, biophysics and technology of photodynamic therapy. Phys Med Biol. 2008;53(9):R61-R109.